HHS Public Access

Author manuscript

Annu Rev Anal Chem (Palo Alto Calif). Author manuscript; available in PMC 2019 June 12.

Published in final edited form as:

Annu Rev Anal Chem (Palo Alto Calif). 2018 June 12; 11(1): 509–533. doi:10.1146/annurev-anchem-061417-125619.

Methods of Measuring Enzyme Activity Ex vivo and In vivo

Yangguang Ou, **Rachael E Wilson**, and **Stephen G. Weber***

Department of Chemistry, University of Pittsburgh, Pittsburgh, PA, USA

Abstract

Enzymes catalyze a variety of biochemical reactions in the body and, in conjunction with transporters and receptors, control virtually all physiological processes. There is great value in measuring enzyme activity ex- and in vivo. Spatial and temporal differences or changes in enzyme activity can be related to a variety of natural and pathological processes. Several analytical approaches have been developed to meet this need. They can be classified broadly as either methods based on artificial substrates with the goal of creating images of diseased tissue or methods based on natural substrates with the goal of understanding natural processes. This review covers a selection of these methods, including optical, magnetic resonance, mass spectrometry, and physical sampling approaches, with focuses on creative chemistry and method development that make ex vivo and in vivo measurements of enzyme activity possible.

Keywords

MALDI mass spectrometry imaging; Microdialysis; Magnetic resonance; Fluorogenic; Electroosmotic sampling; Electroosmotic push-pull perfusion

1. Introduction

This review mostly focuses on recent literature describing approaches to probing enzyme activity ex vivo and in vivo. We also describe some proof-of-principle experiments that have not been applied ex vivo or in vivo but hold significant potential for such measurements. Methods for qualitative and quantitative measurements of enzyme activity ex vivo and in vivo fall into two broad categories. The main objective may be biochemical or neurochemical, such as understanding the differences in a metabolic pathway in two regions of the brain. Or it may be to reveal, typically by imaging, qualitative differences that exist because a particular enzyme's level of activity is associated with a specific pathology in a particular anatomical region such as a tumor. In this case, the goal is "morphological" (1) as the enzyme's activity defines the size and morphology of the diseased region. The latter type of measurement depends on the use of synthetic substrates. These are chemical probes that undergo a measureable change upon being altered by an enzyme-catalyzed reaction. Fluorescence and magnetic resonance techniques are the major tools for imaging such chemical probes. The biochemical types of investigations may also use chemical probes, but the use of physical probes to introduce substrates and collect substrates and products is also

yao5@pitt.edu, rew66@pitt.edu, sweber@pitt.edu. *Corresponding author information: 603 Chevron Science Center, 219 Parkman Ave, Pittsburgh, PA 15260, 412-624-8520.

common. The use of physical probes is often associated with investigations of the fate of natural substrates lacking a strong detectable tag, so instrumental methods of analysis such a mass spectrometry are important for this type of study. This review emphasizes the biochemical and neurochemical applications.

We begin with a discussion of chemical probes to illustrate the various ways in which researchers have used enzyme activity to produce a measureable signal change. We then take a technique-oriented route to describing key concepts and recent advances in methods for determining enzyme activity in animals (in vivo) and in functional tissue taken from, and representative of, a healthy or diseased animal (ex vivo). There are some examples that do not fit this definition, but that are either historically important (in situ zymography) or recent creative in vitro demonstrations headed for in/ex vivo applications in the future. We cover both chemical probes and physical probes, including microdialysis and electroosmosis-based sampling methods coupled with various separation and detection techniques. It is important to note that this review is by no means meant to be a comprehensive review of the literature as a whole. Many reviews are cited for further information.

2. Measuring Enzyme Activity

2.1 Substrates

Many methods use natural substrates for measurements of enzyme activity. Magnetic resonance spectroscopy (MRS) and imaging (MRI) based on ^{31}P permits the measurement of creatine kinase activity (2) because the signal from ATP and phosphocreatine occur at different chemical shifts. Techniques that acquire substrates and products from tissue, such as microdialysis (e.g., 11β-hydroxysteroid dehydrogenase type 1 (3–5)), electroosmotic push-pull perfusion (e.g., aminopeptidases (6)), or MALDI-MS (e.g., related to dynorphins (7)) may use or measure natural substrates and products. There are many reasons to use natural substrates. The determination of the K_m of an enzyme for a particular substrate may be a goal. In addition, the focus of the research may not only be to identify or quantitate the activity of an enzyme but also to investigate the production and fate of a natural agonist or antagonist that depends on the activity of enzymes in a particular pathway.

There is a class of artificial substrates that provides a signal irrespective of enzyme activity. These are used in imaging applications, by positron emission tomography and single photon emission computed tomography in vivo, for example. In these experiments, enzyme activity acts to trap the probe so it is not excreted rapidly following injection (reviewed for monoamine oxidases (8)). High affinity enzyme inhibitors can act in the same way (9).

Another large class of artificial substrates depends on enzyme activity to turn on a detectable signal that indicates enzyme activity in vivo or ex vivo. Despite the many analytical techniques used to measure a signal generated by a designed artificial substrate, there are similarities among them. (For an excellent review see (10)). We have placed them in four categories based on the physicochemical influence of enzyme action on a substrate: proximity, assembly/disassembly, reactivity, and spectroscopic shift. A small number of examples support the general description in each category below. In several cases, a substrate could be placed in more than one category.

In both fluorescence measurements and magnetic resonance measurements, the proximity of two chemical species can influence the measured signal. Fluorescence quenching and Förster (or "fluorescence") resonance energy transfer, commonly known as FRET, have been used to visualize enzyme activity by connecting a pair of chemical species by a chemical linker that can be broken, e.g., by a hydrolytic enzyme. Proteases cleaving a peptide sequence linking two fluorescent proteins can be determined using the fluorescence change(s) accompanying the physical separation of the FRET pair (reviewed in (11)). A variety of small-molecule probes can be synthesized to accomplish a "turn on" or "turn off" signal based on dynamic or static quenching occurring between two moieties tethered by a cleavable linker (reviewed in (12)). Magnetic resonance techniques can use similar ideas. The Weissleder group (13, 14) discovered that superparamagnetic covalently labeled iron oxide nanoparticles had a dramatically different effect on spin-spin relaxation times of water protons, T_2, when they were aggregated (low T_2) as opposed to freely diffusing (high T_2). Aggregates held together with a linker containing a specific peptide sequence, in this case DEVD, were dispersed in the presence of the enzyme caspase-3 leading to a change in the magnetic resonance signal from water. A similar idea underlies a molecular-scale substrate. If a Gd(III) ion is held near ^{19}F, the latter's T_2 is short. By connecting a Gd-containing complex to a ^{19}F-containing organic moiety through a DEVD-containing peptide linker, a probe sensitive to the presence of caspase-3 was created (15). In the presence of the enzyme, there is an increase in T_2 and a consequent increase in signal intensity.

Assembly of active agents can lead to differences in their physicochemical or spectroscopic properties. One interesting proof-of-principle report (16) provides a highly selective histological image indicating the presence of a *pair* of enzymes, β-galactosidase and leucine aminopeptidase, in a cell line. The imaging agent creates a fluorescent aggregate that precipitates after the hydrolysis reactions occur. Another fluorescent probe was developed to detect the presence of apoptotic cells in tumors (17). In this case, delivery of the probe in vivo was by adventitious transport caused by extravasation into the tumor. Reduction by local glutathione and hydrolysis of a peptide bond by caspase-3 led to macrocycle formation and aggregation of those macrocycles. The aggregation increased fluorescence of the hydroxyquinoline-based fluorescent moiety and inhibited diffusion of the probes out of the (leaky) tumor cells.

Altering a molecule's reactivity can be used for imaging. In a proof-of-principle study, Kwan et al. (18) created derivatives of coumarin which, when hydrolyzed enzymatically, led to a reaction of the product with nearby nucleophiles to form a fluorescing species. In contrast to so-called activity-based probes, in which the product of the enzyme-catalyzed reaction reacts with said enzyme, the foregoing probe's reaction product is not as reactive. Thus, the reaction product reacts with something in the neighborhood but does not inactivate the enzyme, increasing sensitivity over activity-based probes. The application was histological in nature. In a recent report, similar chemistry was used to visualize β-galactosidase-bearing cells in mouse brain tissue (19). An alteration in the rate of exchange of a proton on a molecule with a proton on water can lead to the ability to image the molecule (Figure 1). The change in exchange rate is a change in reactivity, so we include here the technique known as chemical exchange saturation transfer, or CEST (20, 21). The exchange rate of amine protons is much greater than that of amide protons, thus enzymatic

hydrolysis of the amide leads to a greater CEST effect and the ability to image the locale where the enzymatic reaction takes place. This was first done to detect the presence of caspase-3 (22, 23). In recent work, the Pagel group has developed a self-referencing probe with one signal responding to peptidase activity and one not as shown in Figure 1 (24).

Changes in spectroscopic signatures, and especially “turn on” mechanisms, are valuable paths to detection. This idea has been used in the imaging of enzyme activity by creating a synthetic pro-fluorophore that is uncaged by an enzyme to react intramolecularly to form an active fluorophore. Gu et al. (25) employed this strategy to visualize β-galactosidase-containing tumor cells. The enzyme, by cleaving the galactose ester profluorophore, created near infrared fluorescence that could be imaged in mice.

2.2 Optical, Magnetic Resonance, and Nuclear Imaging Methods

2.2.1 Fluorescence-based methods—The applications of fluorescence techniques are geared towards clinical imaging. As a result, the majority of the work in this area is based on single-photon near infrared (NIR) or two-photon measurements. The lower scattering propensity of the longer wavelengths of light allows the ability to image deeper into the tissue. There is a rich literature on FRET and quenching phenomena being applied to biochemical problems. Researchers have taken advantage of that for design of probes, however additional, significant ingenuity has gone into the overall probe design to improve other meritorious attributes including delivery, signal integrity, and enzyme selectivity. The majority of applications have been to determine a particular protease activity with examples of applications in arthritis (26), ischemia (27–30), and cancer (17, 25, 31, 32).

In situ zymography (ISZ) (33, 34) is a histological technique that provides an image indicative of matrix metalloproteinase (MMP) activity. (We note here that it uses frozen or fixed tissue slices, so we do not consider it to be an ex vivo preparation. We include it because of its increasingly broad application and high information content.) ISZ is both similar to and different from the conventional immunohistochemistry method. The latter provides an image reflecting quantitative estimate of an epitope, while ISZ reports on spatially resolved quantification of active enzymes. ISZ is almost exclusively used to measure activity of MMPs, which degrade the extracellular matrix. Since MMPs facilitates metastasis, a primary application of ISZ is for cancer studies. Enzyme activity is visualized with a microscope. Historically changes in color, and more recently changes in fluorescence, occur due to MMP activity following the placement of a tissue slice on a microscope slide with an MMP substrate. Substrates are protein-based, e.g., gelatin, casein, and others (35). (In fact, the enzymatic activity can be referred to by a substrate-based name, e.g. gelatinase activity, rather than a class-based name, e.g., MMP-2 and MMP-9.) In the first human brain study using ISZ on stroke victims, the use of fluorogenic MMP substrates with different selectivity showed that there was elevated MMP-9 activity in the infarct core near blood but that MMP-2 activity was not affected (27). Despite the success of this technique, the need to use unfixed frozen sections resulted in loss of fine structure with concomitant degradation of spatial resolution, which precluded investigations of MMP activity at the synaptic level, such as in synaptic plasticity. Thus, Gawlak et al. strove to achieve better resolution, down to diffraction limit of light ~200 nm (36). They fixed hippocampal tissue in a methanol/ethanol

mixture, which preserves enzyme activity (37), followed by embedding in polyester wax, which preserved the fine structure. Slices from the wax-embedded tissue were de-waxed with ethanol. Using this method, they identified synapses containing specific excitatory glutamate receptors with gelatinase activity. They determined that glutamate receptor-associated gelatinase activity increases with seizures. Hadler-Olsen developed a similar approach using ethanol- and zinc-buffered fixed tissues in paraffin-embedded wax (38). Fixing the tissues also allowed for coupling of ISZ to other techniques, such as SDS-PAGE and Western blotting. Recently, ISZ coupled with immunoblotting and immunofluorescence revealed that MMP-3 inhibition prevented induction of L-type voltage gated calcium channel-dependent long-term potentiation (LTP) in the hippocampus but had no effect on NMDA-dependent LTP (39). The latter depends solely on MMP-9 activity (39). This study provided more mechanistic information on the role of MMPs in synaptic plasticity and learning.

The development of protease-activated fluorogenic probes led to the development of in vivo methods. Early work relied on nonspecific substrates for measuring general proteolytic activity (32) but more specific biocompatible fluorogenic MMP substrates as reporter probes have been developed (40). The Weissleder group first published on using fluorescence to signal the presence of certain enzyme activity in vivo (32). The probe was based on a poly-lysine backbone, chemically modified with poly(ethyleneglycol) segments and the fluorophore Cy5.5. Until the poly-lysine backbone is hydrolyzed by a protease, fluorescence from the Cy5.5 is quenched. Based on inhibitor experiments, the selectivity of the probe is for lysosomal cysteine and serine proteases. Tumors grown in mice were detected by imaging 24 h after injection of the probe. To build in more selectivity, the group attached the fluorophore to the backbone through a peptide sequence favored by cathepsin D (41). This probe was use to image tumors implanted in mice. Another probe is based on covalently labeled iron oxide nanoparticles which quench, but do not eliminate, fluorescence (42). Two non-interacting (with each other) fluorophores were appended to the nanoparticles, Cy5.5 through a protease-susceptible tetra-arginine linker and Cy7 directly. Tumors grown in mice were effectively visualized based on the measurement of the ratio of the fluorescence signal from Cy5.5 to that of Cy7 as enzymatic hydrolysis of the tetra-arginine linker turned on Cy5.5 fluorescence but had only a very small effect on the Cy7 fluorescence. The “unquenching” of the Cy5.5 fluorescence is due to its liberation from the nanoparticle not from nearby Cy7.

A classical zymography substrate is DQ-collagen with the label “DQ” implying that the protein is modified heavily with fluorescent tags that quench each other due to their proximity. Keow et al. (43) replaced the DQ-collagen with FRET-quenched fluorophores as substrates for in vivo zymography. In this case, a fluorophore and quencher moiety are separated by 10-amino-acid long linker sequence, which, when cleaved, results in fluorescence signal. The benefit of this modification is that there is greater control over the linker sequence, thereby allowing for better enzyme specificity. Moreover, different fluorophore/linker pair with different spectroscopic properties can be used simultaneously to detect multiple enzyme activities in the same tissue (43). The authors coined the term “differential in vivo zymography” for this technique. Vandooren et al. provides a detailed review of all zymography techniques (35).

In the foregoing fluorescence-based techniques, the enzyme activity and its identification with particular anatomical structures are generally the focus of the measurements. It is also possible to focus on the spatial and temporal changes in anatomically defined enzyme activity during development. With proper treatment of the tissue, ex vivo measurements can have diffraction limited spatial resolution and the enzyme activity imaged can also be identified with particular proteins by immunohistochemistry. The focus on extracellular proteases has advanced knowledge of extracellular processes related to synaptic plasticity and matrix remodeling (44).

Many other enzyme classes have been imaged using fluorescence. Activity-based fluorescent probes label active enzymes out of all enzymes present. These probes can be used for imaging in vivo due to the faster elimination of the unreacted probe than the labeled enzyme. Lee et al. (45) optimized the chemistry of an existing Cy5-based probe for a cysteine protease, legumain (asparaginyl endopeptidase), to make it function in imaging applications. The cellular uptake and enzyme selectivity were improved over an earlier design that had shown promise in vitro but was not very effective for in vivo imaging. An important conclusion was that increasing cellular uptake did not necessarily improve the imaging. Another way to image is for an enzyme to cause a signal-producing precipitate. Prost and Hasserodt (16), in a proof-of-principle study, created a substrate that requires both β-galactosidase and leucine aminopeptidase in order to form a reactive carbamate of a phenol-containing fluorophore. The carbamate undergoes an intramolecular cyclization/elimination reaction to reveal the phenol, which precipitates and fluoresces. The probe has clear histological applications. Gu et al. created a turn-on fluorescent substrate that is ratiometric, which improves data quality. The small-molecule pro-fluorophore was used to image tumors in mice based on sensitivity to β-galactosidase, although it does not appear that the imaging process took advantage of the ratiometric property of the label (25).

Fluorescence techniques have many advantages not the least of which is the remarkable variety of fluorescent molecules and means to alter fluorescent quantum yield that provide routes to signal- or image-producing techniques. The synthetic chemistry required to make them reactive – as labels – is also very mature. Using NIR radiation makes imaging of fluorescent probes practical. There are limitations, such as the effect of a local environment of fluorescence lifetime, which may alter signals quantitatively. However, for some imaging applications this may not be a significant problem.

2.2.2 Magnetic resonance-based methods—A considerable amount of early work was carried out to investigate metabolism and metabolic pathways using MRS (46, 47). In a widely used type of experiment, the same nucleus may be found on more than one chemical species leading to exchange. One example of this involves the use of the naturally occurring, NMR-active nucleus, ^{31}P (48). The intracellular inorganic phosphate created from magnetically saturated ATP in yeast can be determined leading to a reaction rate measurement (49). In this type of investigation, known as saturation- or magnetization transfer, the overall reaction may involve several participating enzymes because the tracked species are cofactors participating in many reactions. There is also a requirement that the relaxation time for the chemical reaction(s) must be similar to the nuclear spin relaxation time in order for them to be visualized by this technique. The flux through key energy-

related pathways governed by ATP synthase and creatine kinase can be determined in muscle tissues in vivo using ^{31}P MRS. ^{15}N is, on the other hand, very low in abundance, thus the infusion of ^{15}N-labeled precursors allows one to measure the changes in abundance of reaction products. Glutamine synthetase has been the focus of this approach in brain where the glutamine/glutamate cycle is important (50). Rates of the enzyme catalyzed reaction can be inferred from an isotope chase experiment. In this approach, the MRS measurement shows a steady state concentration of ^{15}N-labeled glutamate while infusing a constant concentration of $^{15}NH_4Cl$, then the infusate was switched to $^{14}NH_4Cl$ and the exponential decline in (5-^{15}N)glutamate signal was measured. A key aspect of the glutamine/glutamate cycle is the rate of glutamine export from glia that occurs through system A transporter 3 (SNAT3). In an elegant study Kanamori and Ross combined ^{15}N-glutamine flux measurements with microdialysis measurements of extracellular glutamine to infer the intra/extracellular glutamine gradient required to export glutamine to the extracellular space (51). In another type of experiment, isotope labeling is used and substrate and product(s) are measured. The signal from^{1}H, ^{13}C, or ^{15}N on a substrate will appear on a ^{2}H-, ^{12}C-, or ^{14}N- containing metabolic product. The rate of the process can thus be inferred directly (52).

The establishment of imaging techniques and the use of abundant nuclei such as ^{1}H (including water protons), ^{19}F, and ^{31}P as the bases for the signal has increased the scope of magnetic resonance to include the investigation of pathology based on determining the activity of enzymes that catalyze a particular reaction in vitro and in vivo. Particularly powerful and common is the use of signals from protons on the water and fat molecules because they are abundant and imaging instruments are typically set up for this nucleus. The first report of an enzyme-activity-targeted measurement for MRI used contrast agents that contain Gd(III) (53, 54). The enzyme β-galactosidase was the target. This enzyme is used widely to determine transcriptional regulation following insertion of the *LacZ* gene. Thus, the Meade group applied their Gd-based substrate to β-galactosidase imaging in a *Xenopus* embryo following injection of the *LacZ* gene (54). The substrate's design took into account the mechanism by which Gd(III) chelates create contrast, which is by altering water proton longitudinal relaxation time, T_1. As a consequence, blocking a water coordination site alters the chelate's relaxivity, thereby changing the contrast (53). The substrate, when hydrolyzed, unblocked a water coordination site and consequently the enzyme activity could be visualized. Note that the effect of such an agent on a spectrum or image depends on parameters other than the relaxivity, notably the concentration of the agent and the applied magnetic field. The effect of superparamagnetic nanoparticles on the transverse relaxation time, T_2, of water protons depends on their state of aggregation and/or proximity to each other. As a result, cross-linked iron oxide nanoparticles (CLIOs) are effective substrates for imaging if they can be made to aggregate or dissociate. A protease-sensitive substrate was created by linking CLIOs to both ends of a peptide sequence that is a protease substrate (55). The unhydrolyzed substrate aggregates while the hydrolyzed products do not. The resulting changes in relaxivity lead to contrast.

Fluorine has been used as a label to determine enzyme activity based on a simple chemical shift that results from the enzymatic reaction (56) and also in a more general platform in which an enzyme cleaves a bond that allows a Gd-labeled portion of the substrate to diffuse

away from the ^{19}F-labeled portion. The separation of the ^{19}F-labeled substrate from the paramagnetic Gd increases T_2 and increases contrast (15).

Magnetic resonance-based methods have many advantages for in vitro and in vivo determination of enzyme activity. Depending in the specific techniques used, these advantages include a high degree of chemical specificity in the measurement of a substrate or product, being non-invasive, and providing images. Excellent recent reviews can be consulted for more details (57–61).

2.3 Mass spectrometry-based methods

With the advent of MALDI 30 years ago (62), mass spectrometry imaging (MSI) techniques have become an increasingly popular method for measuring enzymatic activity. For historical context, the reader is directed to a 2007 review by Greis (63). The use of novel surface materials and ionization techniques such as surface-assisted laser desorption/ionization (SALDI), nanostructure-initiator mass spectrometry (NIMS), and self-assembled monolayers for matrix-assisted laser desorption/ionization (SAMDI) have allowed the development of high-throughput enzymatic assays to screen inhibitors and determine enzyme/inhibitor kinetics. They are often coupled with time of flight (TOF) mass analyzers, which offer high resolution and a wide mass range. More information about these applications can be found in a review by de Rond (64). In terms of studying enzymatic processes for understanding biochemistry and neurochemistry, perhaps the greatest power of MALDI is high spatial resolution. This is especially important in neurological applications since the function of a particular enzyme is often tied to its location in a specific brain region (7). Furthermore, this can rely on natural substrates and products making it more amenable to tissue-based studies (7). A drawback, however, is that analytes are ionized directly from a surface without any separation step, resulting in bias for high intensity signals (65). This is especially an issue for low abundance substrates such as endogenous peptides. Additionally, obtaining sequence information about these peptides comes at a cost of instrument time and spatial resolution (65), limiting the utility of this technique for the discovery of novel endogenous substrates. OuYang, et al. have addressed these challenges using a novel multiplexing technique along with MALDI-LTQ-Orbitrap XL to perform data dependent acquisition (DDA) of endogenous neuropeptides in blue crab (*Callinectes sapidus*) brain tissue slices (65). By sequentially performing full scan MS followed by DDA in spiral steps at each raster position (Figure 2), analyte sequence information was obtained while preserving spatial resolution (65). Furthermore, the authors expanded the four-step spiral method depicted in Figure 2 to a nine-step method, where the entire mass range was broken down into three narrower mass ranges, which were scanned in Steps 1, 4, and 7. Steps 2/3, 5/6, and 8/9 were data-dependent fragmentations of the top 2 ions in each preceding full scan. By dividing the full scan mass range into fractions prior to DDA, the authors were able to identify one novel and 38 known endogenous neuropeptides using a structural database (65).

The ability to spatially identify specific and even unknown peptides holds great power in identifying relevant enzyme substrates and thus enzyme function. Peptide hydrolysis can be studied *in situ* by incubating tissues with substrate with or without inhibitor. MALDI-TOF is

used to detect substrate and hydrolysis product ions which can be used to create a map of enzyme activity (66). This technique has been used along with in vitro analyses of tissue homogenates to study the degradation of angiotensin in the mouse kidney (66). Combining *in situ* histochemistry with mass spectrometric imaging, the Andersson group has demonstrated the production of different hydrolysis products of the neuropeptide dynorphin B in different regions of the rat brain. After applying inhibitor to one side of a brain tissue slice followed by dynorphin B across the entire tissue, the authors used MALDI to investigate the effects of several inhibitors, including N-ethylmaleimide (inhibits cysteine peptidases), phosphoramidon (inhibits metallo-endopeptidases) and opiorphin (inhibits Zn-ectopeptidases, aminopeptidase N (APN), and neutral endopeptidase (67)) on dynorphin B hydrolysis. As seen in Figure 3, it was found that certain dynorphin B fragments, including dynorphin B (1–7) and dynorphin B (2–13), had higher relative intensities in the cortex and striatum, respectively, and that each of the inhibitors had differing effects on the fragments that were generated. This is relevant to the study of Parkinson's associated dyskinesia, which has been correlated with elevated levels of dynorphin B in the striatum and substantia nigra, two regions which also show differential rates of dynorphin B hydrolysis (7).

While a major advantage of MALDI is the ability to detect unlabeled substrates, activity-based tags can be used for difficult to detect analytes, including enzymes (68). With this approach, an enzyme-specific, alkyne-containing, activity based probe is applied to formaldehyde-fixed tissues. Following the probe's binding to the active site of the enzyme, a laser-cleavable mass tag applied to the tissue reacts with the probe via click chemistry. In this approach, the laser beam releases the mass tag from the sample. Thus, the relative intensity of the signature mass can be correlated with the activity of the enzyme. Because no matrix is required, spatial resolution is only dependent on the diameter of the laser beam (20–50 μm) and hundreds of tags can be linked to one clickable probe, resulting in significant signal amplification. These advantages allow the study of enzymes that are not typically accessible to traditional MALDI study including membrane-bound peptidases. The method has been used successfully to map the location of serine hydrolases in rat brain and mouse embryo tissue slices (68).

Mass spectrometry's effectiveness in measuring the activity of diverse enzymes is to a large degree due to the mass selectivity of the technique. Isomerases, for example those enzymes that convert L-amino acids to D-amino acids, yield a product with the same mass as the substrate. Nonetheless, there are methods that are sensitive to the presence of D-amino acid-containing peptides (DAACPs). In MALDI-TOF/TOF, the presence of a D-amino acid in the peptide chain has sequence-dependent effects on fragmentation. (69) This effect can be used for targeted studies because differences in the fragmentation of an all L-amino acid peptide standard and that of a peptide containing a D-amino acid can be used to identify where the isomerization has occurred. (69) However, this limits the number of peptides that can be studied simultaneously and is not conducive to the discovery of endogenous DAACPs since prior knowledge of substrate identity is required. (70) Another approach known as the "DAACP discovery funnel" allows a sample first to be screened for DAACPs using APN. APN hydrolyzes non-DAACPs much more rapidly than DAACPs (70). Peptides that survive 48 h exposure to APN based on MALDI-TOF/TOF analysis are potential DAACPs. These non-hydrolyzed peptides are acid hydrolyzed into individual amino acids with deuterium

chloride and derivatized with Marfey's reagent (1-fluoro-2,4-dinitrophenyl-5-L-alanine amide), which labels the α-amino group of each amino acid with L-alanine amide. (71, 72) The resulting diastereomeric D-and L-amino acid-containing dipeptides can then be separated and detected by LC-MS. (70) Based on the knowledge of which D-amino acids are present and their suspected position, DAACPs are then synthesized and analyzed by LC-MS/MS. Confirmation of the identification of endogenous peptides are made by comparison with retention times of the synthesized DAACPs. This method was used to identify novel DAACPs in the pedal ganglia of *Aplysia californica*, one of which was bioactive whereas the other was not. Thus, this approach is promising for the discovery of endogenous DAACPs regardless of bioactivity but does require the D-amino acid to be located near the N-terminus.

2.4 Sampling-based methods

2.4.1 Microdialysis—The most widely used in vivo sampling method is microdialysis (73) (Figure 4), in which species, such as substrates and products, can diffuse through the semi-permeable membrane comprising the probe. Thus substrates can be introduced locally to the tissue and diffusing components of the extracellular space (ECS) can be collected, identified, and/or quantified. Probes have dimensions typically 1 – 4 mm long and a diameter of ~250 μm, which limits the spatial resolution and the regions that can be studied by the method. Microfabricated probes have recently been developed to improve spatial resolution (74). The main appeal of microdialysis is its breadth, both in the ease of coupling to separation and detection methods as well as the variety of enzyme systems it can probe.

In vivo microdialysis can be used to follow enzymatically catalyzed transformation of small, active molecules in the brain and monitor inhibitor/drug efficacy. In a typical experiment, there is a stabilization period before any samples are collected for quantitation. Perfusion of the probe with drugs or inhibitors, a process called retrodialysis, is often done in conjunction with sampling from ECS. In one study, in vivo microdialysis measured elevated extracellular glutamate concentration in the periphery of the injured region after focal cerebral ischemia (75). Retrodialysis with glutaminase substrate glutamine and activator phosphate resulted in further elevation of extracellular glutamate, indicating that increased glutaminase activity may contribute to excess extracellular glutamate. In another study, microdialysis was used to sample adenosine, which is formed from dephosphorylation of adenosine monophosphate, a reaction catalyzed by ecto-5'-nucleotidase (76, 77), a membrane-bound enzyme whose catalytic domain faces the ECS. Lysophosphatidylcholine (LPC) administration significantly increased ecto-5'-nucleotidase activity, as evidenced by increases in adenosine concentration in the dialysate, whereas perfusing the probe with a protein kinase C antagonist abolished this elevation. This led to the proposal that LPC results in elevated ecto-5'-nucleotidase activity through a protein kinase C pathway. Microdialysis has also been used to investigate the role of 11β-hydroxysteroid dehydrogenase activity (11βHSD) in obesity and diabetes (3–5). 11βHSD type 1 (11βHSD 1) can catalyze the reduction of cortisone to cortisol in the presence of NADPH. It was demonstrated in the literature that 11βHSD1 knockout mice on a high-fat diet are rescued from obesity and hyperglycemia (3). Thus, Sandeep et al. infused the subcutaneous adipose tissue of human patients with 1,2,6,7-[^{3}H]-cortisone and measured 1,2-[^{3}H]-cortisone and 1,2[^{3}H]-cortisol concentrations in the dialysates (3). 11βHSD1 activity was inferred from the steady-state concentrations of the two species using unlabeled

cortisol and cortisone as internal standards. It was found that obese subjects had more rapid conversion of [^{3}H]-cortisone to [^{3}H]-cortisol, indicating higher 1βHSD1 activity, in agreement with previous findings.

Microdialysis has the ability to study the fate of multiple substrates simultaneously. This has been demonstrated in the study of MMPs wherein two microdialysis probes were implanted in the subcutaneous space on either side of the rat dorsal spine of freely moving animals (78). Each probe was perfused with MMP-1 and MMP-2/-9 substrates by retrodialysis. MMP-2 and MMP-9 share the same substrates and thus cannot be distinguished. They found N-terminal product concentrations of MMP-1 and MMP-2/-9 substrates stabilized around 90 min at 2.6 μM and 3.1 μM, respectively. Retrodialysis of the broad-spectrum MMP inhibitor GM 6001 reduced MMP-1 activity by 29% and MMP-2/-9 activity by 22%. Intact substrate along with enzymatic products were detected using LC-MS/MS (78). Zymography of tissue encapsulating the probe versus that of healthy tissue revealed elevated MMP activity near the probe, suggesting perturbations to the tissue due to the presence of the probe (78). This is in agreement with other findings that the microdialysis probe implantation causing a significant foreign body response (79), which in the short term could influence measurements and in the longer term results in scar tissue surrounding the probe and reducing the probes recovery of species in the ECS. Fortunately, recent strategies have been developed that show promise in minimizing the effect of the probe on the tissue, including retrodialysis of the anti-inflammatory glucocorticoid dexamethasone (80–84).

Another advantage of microdialysis is the ability to analyze metabolic processes in an awake, behaving animal. This allows the study of peptidases that may have behavioral effects, such as insulin regulated aminopeptidase (IRAP). Inhibition of IRAP by the peptides angiotensin IV and LVV-haemorphin 7 has been shown to have a positive effect on memory in rats (85). Additionally, IRAP may also affect glucose levels in the extracellular space (86). Using microdialysis to monitor glucose levels in the rat hippocampus throughout behavioral testing with and without intracerebroventricular treatment of IRAP inhibitors, it was found that IRAP inhibition had a positive effect on spatial working memory while glucose levels were unaffected (87). A similar approach has also been used to demonstrate the effects of these peptide inhibitors on acetylcholine levels in the rat hippocampus (88).

One drawback of microdialysis is low recovery, particularly for peptides. Approaches to addressing this problem include the addition of affinity agents such as cyclodextrins or antibodies in the perfusate to improve mass transport across the membrane (89–91). Nonetheless, microdialysis has been demonstrated to be a versatile technique for the study of a variety of substrates and metabolites, including but not limited to substance P (92), *β*-endorphin (93), dynorphin A (94, 95), angiotensin II (96), and peptide E (97).

2.4.2 Electroosmosis-based methods—Electroosmosis (EO) is the bulk fluid movement that occurs when an electric current is passed through electrolyte-filled conduits with charged walls, e.g. fused-silica capillaries (98) and the brain ECS (99). There are two generations of EO-based sampling techniques for measuring enzyme activity ex vivo in tissue cultures, as described below. All of the work done is on organotypic hippocampal

slice cultures (OHSCs), which are prepared from postnatal 7-day-old Sprague Dawley rat pups (100).

A typical experiment in the first generation of EO sampling consists of positioning the proximal end of a fused silica (sampling) capillary on top of an OHSC with the distal end in an electrode-containing vessel. A second electrode was placed in the same bath as the OHSCs to complete the circuit. The electrodes are connected to a current source. Exogenous substrates may be added to the bath underneath the tissue culture. Upon application of a current, fluid flows from the bath beneath the culture, through the tissue culture, and into the sampling capillary. Membrane-bound enzymes whose catalytic domains face the ECS can hydrolyze substrates carried by EO flow. The activity of these enzymes, called ectopeptidases, has been of great interest in recent years when it was discovered that they regulate the bioactivity of important peptides involved in growth, cell survival, and stress responses (reviewed in Ou et al. (98)). Several such as dipeptidylpeptidase IV, and neutral endopeptidase have also become important therapeutic targets (101–103).

The first generation of EO sampling was integrated with microfluidic capillary electrophoresis coupled to confocal laser-induced fluorescence detection (Figure 5a) (104, 105). The distal end of the sampling capillary is attached directly to the microfluidic device. Collected thiol compounds react with ThioGlo-1 dye in the reaction channel before separation. This method was used to measured endogenous free cysteine (11.1 ± 1.2 μM), homocysteine (0.18 ± 0.01 μM), and cysteamine concentrations (10.6 ± 1.0 nM) in the ECS of the OHSCs (105). Cysteamine (CSH) is the active terminal product of synthesis and degradation of coenzyme A (CoA, Figure 5c), an important cofactor for 4% of all enzymes (105). Wu et al. perfused the CA3 region of OHSCs with CoA and monitored changes in CSH and pantetheine (PSH) concentrations (an intermediate in CoA catabolism) in the ECS using the integrated method described above (104, 106). Typical reaction time for these experiments was estimated by dividing the total effective volume of the tissue (taking into account the porosity of the medium) by the flow rate and was determined to be 55 s. Plotting CSH concentration generated a function of CoA concentration yielded a nonlinear Michaelis-Menten curve, from which the overall reaction rate of the CoA → CSH can be extracted (Figure 5b). Wu et al. reported an apparent V'_{max} = 7.1 ± 0.5 nM/s and K'_m = 16 ± 4 μM for the overall enzymatic degradation of CoA in the CA3. Furthermore, fitting the Michaelis Menten equation to the plot of generated pantetheine as a function of CoA concentration revealed a comparable K'_m for pantetheine (18 ± 6 μM) to that for CoA → CSH (Figure 5b). This suggests that the final process in the CoA catabolism pathway, catalyzed by patetheinase, is not the rate-limiting step and is in the first-order regime. These reports provide the first rates of pantetheine and cysteamine formation in mammalian tissues, which had not been reported prior to this work due to lack of appropriate tools that can measure low endogenous concentrations. The authors also administered the disulfide forms of cysteamine, cystamine, and pantethine, pantetheine, two drugs that treat cystinosis, an autosomal recessive genetic disease that cause cysteine to accumulate in lysosomes. Cysteamine is the active molecule in the treatment of cystinosis. Wu et al. (104) found that cysteamine is more rapidly produced from cystamine than pantethine, which agrees with the higher efficacy of cystamine in treating cystinosis. Since cysteamine is toxic in high doses,

the rapid production of cysteamine from cystamine also agrees with findings that cystamine is more toxic than pantethine.

EO sampling has also been coupled to offline capillary liquid chromatography (cLC) with electrochemical detection (107). Rather than being coupled to a microfluidic device, the sampling capillary is removed from the OHSC after sampling is complete and the contents are ejected using a syringe containing 0.1% trifluoroacetic acid (TFA) to quench any enzyme reaction if enzymes were collected in the sampling process. The samples were analyzed with capillary liquid chromatography, reacted with biuret reagent to make the peptides electrochemically active in a postcolumn reactor, and detected with amperometry at a carbon fiber microelectrode. Xu et al. used this method to measure the rate of Leu-enkephalin (YGGFL) hydrolysis in whole OHSCs. They found the major hydrolysis product to be GGFL. As the solute residence time in the cultures is short (seconds), the assumption that the initial substrate concentration does not change can be used. Thus the Michaelis-Menten equation can be applied to these measurements. Inhibitor experiments indicate that the peptidase is likely to be bestatin-sensitive aminopeptidase, with V_{max} = 770 ± 95 μM/s and K_m = 1.2 ± 0.5 mM. Product generation was unaffected by GEMSA, captopril, and puromycin. Ultimately, the objective of this work is to map differences in enzyme activity in brain regions over time or after injury. Thus the precision of the V_{max} determination is encouraging.

To improve spatial resolution, the substrate was introduced through a second pulled capillary near the sampling probe's proximal end (Figure 6). This second-generation EO-based sampling technique is called electroosmotic push-pull perfusion (EOPPP) (108). *In silico* experiments determined the spatial resolution of this technique to be ~100–300 μm, depending on the applied current (109). Rupert et al. coupled this technique with offline MALDI mass spectrometry to qualitatively determine the differences in galanin hydrolysis patterns in CA1 and CA3 of the OHSCs. Galanin is a 29mer peptide that reduces glutamate concentration after ischemia and is protective against glutamate-induced damage (110, 111). At both short and long reaction times, there was a significantly higher probability of finding short peptides with intact carboxy terminus (indicating aminopeptidase activity) in the CA3. At short but not long reaction times, there was a higher probability of finding long peptides with intact carboxy terminus in the CA3.

In EOPPP, the substrate concentration varies in the tissue culture significantly. In addition, as the source is like a point source, there is a distribution of times that the substrate spends in the culture (Figure 6). The standard Michaelis-Menten equation does not apply. Thus, a finite element model was developed to guide experimental design and data analysis for EOPPP in order to determine quantitative enzyme kinetic parameters. In experiments and calculations, we use a D-amino acid internal standard, $^{D}Y^{D}AG^{D}F^{D}L$, at the same concentration as the substrate, YGGFL. This internal standard is ideal because it has a similar diffusion coefficient as the substrate of interest and it cannot be hydrolyzed by enzymes in the tissue. Through simulations, residence time distribution of the internal standard was measured. Simulations of experiments (Figure 6) demonstrate that there are no differences in the enzyme kinetic parameters determined either using the full residence time distribution or the average residence time. The simulations also showed that a first estimate

of enzyme kinetic parameters, V_{max} and K_m, can be determined from fitting the integrated form of the Michaelis Menten equation (112, 113) to the total product generated (normalized to internal standard) as a function of the initial substrate concentration in the source capillary. However, these first values are not the actual V_{max} and K_m in the tissue ECS because the substrate is diluted significantly in the tissue. A large set of experimental simulations was carried out to determine that a simple numerical factor related the first, observed, values to the actual values (109).

It is known that the CA1 region of the hippocampus is more vulnerable to ischemic damage than the CA3 region but the exact mechanism is still unknown. Ou and Weber hypothesized that different rates of hydrolysis of enkephalins in the two regions, i.e. V_{max} of the aminopeptidase, contribute to this selective vulnerability. GGFL was found to be the main hydrolysis product (107, 114). Using the procedures described above with a range of initial substrate concentrations, S_0, from 0.2 to 2.2 mM yielded V_{max} and K_m of 3.1 ± 0.6 μM/s and 70 ± 40 μM in the CA3 region and 9 ± 1 μM/s and 100 ± 70 μM in the CA1 (114). In the presence of the aminopeptidase inhibitor bestatin, GGFL production was suppressed in both regions and the apparent K_m increased. This is consistent with a competitive inhibitor. Inhibiting the aminopeptidase activity of the neuroprotective YGGFL selectively decreased cell death in the CA1 region following oxygen-glucose deprivation, an *ex vivo* stroke model (114).

One of the benefits of EO-based sampling methods is that cell lysis from the sampling procedure is minimal (99, 115), thereby minimizing the effect of cytosolic enzymes. The technique is more sensitive to extracellular processes than intracellular processes. No significant hydrolysis occurs within the sampling capillary (107). In both generations of EO-based sampling methods, the V_{max} values of the enzymes are the main focus of the studies. Specifically, the method has been used to uncover spatial differences in enzyme activity as well as elucidate the role of the enzyme in various processes such as metabolism and ischemia. Unlike microdialysis, EO-based methods can report quantitative Michaelis Menten parameters V_{max} and K_m. Like microdialysis, both EO-based sampling methods have the appeal of breadth, both in terms of being able to couple to various quantitative detection methods as well as being to study a variety of enzyme systems.

Acknowledgements

This work is supported by NIH R01 GM044842. We thank Professor Mark D. Pagel from University of Arizona for kindly providing the images for Figure 1, Professor Lingjun Li from the University of Wisconsin – Madison for kindly providing images for Figure 2, and Professor Malin Andersson from Uppsala Vanderbilt Lund University for kindly providing images for Figure 3.

Literature cited

1. Van Noorden CJF. 2010 Imaging enzymes at work: Metabolic mapping by enzyme histochemistry. J. Histochem. Cytochem. 58: 481–97 [PubMed: 20124092]
2. Li Z, Qiao H, Lebherz C, Choi SR, Zhou X, et al. 2005 Creatine Kinase, a Magnetic Resonance-Detectable Marker Gene for Quantification of Liver-Directed Gene Transfer. Human Gene Therapy 16: 1429–38 [PubMed: 16390274]

3. Sandeep TC, Andrew R, Homer NZM, Andrews RC, Smith K, Walker BR. 2005 Increased in vivo regeneration of cortisol in adipose tissue in human obesity and effects of the 11β-hydroxysteroid dehydrogenase type 1 inhibitor carbenoxolone. Diabetes 54: 872–79 [PubMed: 15734867]
4. Meas T, Carreira E, Wang Y, Rauh M, Poitou C, et al. 2010 11β-hydroxysteroid dehydrogenase type 1 of the subcutaneous adipose tissue is dysregulated but not associated with metabolic disorders in adults born small for gestational age. J. Clin. Endocrinol. Metab. 95: 3949–54 [PubMed: 20519348]
5. Dube S, Norby BJ, Pattan V, Carter RE, Basu A, Basu R. 2015 11β-hydroxysteroid dehydrogenase types 1 and 2 activity in subcutaneous adipose tissue in humans: implications in obesity and diabetes. J. Clin. Endocrinol. Metab. 100: E70–E76 [PubMed: 25303491]
6. Rupert AEO Y; Sandberg M; Weber SG 2013 Electroosmotic Push-Pull Perfusion: Description and Application to Qualitative Analysis of the Hydrolysis of Exogenous Galanin in Organotypic Hippocampal Slice Cultures. ACS Chemical Neuroscience 4: 838–48 [PubMed: 23614879]
7. Bivehed E, Stroemvall R, Bergquist J, Bakalkin G, Andersson M. 2017 Region-specific bioconversion of dynorphin neuropeptide detected by in situ histochemistry and MALDI imaging mass spectrometry. Peptides *(N. Y., NY, U. S.)* 87: 20–27 [PubMed: 27840228]
8. Brooks AF, Shao X, Quesada CA, Sherman P, Scott PJH, Kilbourn MR. 2015 In Vivo Metabolic Trapping Radiotracers for Imaging Monoamine Oxidase-A and -B Enzymatic Activity. ACS Chem. Neurosci. 6: 1965–71 [PubMed: 26393369]
9. Cumming P, Vasdev N. 2012 The Assay of Enzyme Activity by Positron Emission Tomography. Neuromethods 71: 111–35
10. Razgulin A, Ma N, Rao J. 2011 Strategies for in vivo imaging of enzyme activity: an overview and recent advances. Chem. Soc. Rev. 40: 4186–216 [PubMed: 21552609]
11. Frommer WB, Davidson MW, Campbell RE. 2009 Genetically encoded biosensors based on engineered fluorescent proteins. Chem. Soc. Rev. 38: 2833–41 [PubMed: 19771330]
12. Johansson MK, Cook RM. 2003 Intramolecular dimers: a new design strategy for fluorescence-quenched probes. *Chem.-* Eur. J. 9: 3466–71 [PubMed: 12898673]
13. Josephson L, Perez JM, Weissleder R. 2001 Magnetic Nanosensors for the Detection of Oligonucleotide Sequences. Angewandte Chemie International Edition 40: 3204–06 [PubMed: 29712059]
14. Perez JM, Josephson L, O'Loughlin T, Hoegemann D, Weissleder R. 2002 Magnetic relaxation switches capable of sensing molecular interactions. Nat. Biotechnol. 20: 816–20 [PubMed: 12134166]
15. Mizukami S, Takikawa R, Sugihara F, Hori Y, Tochio H, et al. 2008 Paramagnetic Relaxation-Based 19F MRI Probe To Detect Protease Activity. J. Am. Chem. Soc. 130: 794–95 [PubMed: 18154336]
16. Prost M, Hasserodt J. 2014 "Double gating" - a concept for enzyme-responsive imaging probes aiming at high tissue specificity. Chem. Commun. *(Cambridge, U. K.)* 50: 14896–99
17. Ye D, Shuhendler AJ, Cui L, Tong L, Tee SS, et al. 2014 Bioorthogonal cyclization-mediated in situ self-assembly of small-molecule probes for imaging caspase activity in vivo. Nat. Chem. 6: 519–26 [PubMed: 24848238]
18. Kwan DH, Chen H–M, Ratananikom K, Hancock SM, Watanabe Y, et al. 2011 Self-Immobilizing Fluorogenic Imaging Agents of Enzyme Activity. Angew. Chem., Int. Ed. 50: 300–03, S00/1-S00/35
19. Doura T, Kamiya M, Obata F, Yamaguchi Y, Hiyama TY, et al. 2016 Detection of LacZ-Positive Cells in Living Tissue with Single-Cell Resolution. Angew. Chem., Int. Ed. 55: 9620–24
20. Ward KM, Aletras AH, Balaban RS. 2000 A New Class of Contrast Agents for MRI Based on Proton Chemical Exchange Dependent Saturation Transfer (CEST). J. Magn. Reson. 143: 79–87 [PubMed: 10698648]
21. Sinharay S, Pagel MD, Pagel MD. 2016 Advances in Magnetic Resonance Imaging Contrast Agents for Biomarker Detection. Annu Rev Anal Chem (Palo Alto Calif) 9: 95–115 [PubMed: 27049630]
22. Yoo B, Pagel MD. 2006 A PARACEST MRI Contrast Agent To Detect Enzyme Activity. J. Am. Chem. Soc. 128: 14032–33 [PubMed: 17061878]

23. Yoo B, Raam MS, Rosenblum RM, Pagel MD. 2007 Enzyme-responsive PARACEST MRI contrast agents: a new biomedical imaging approach for studies of the proteasome. Contrast Media Mol. Imaging 2: 189–98 [PubMed: 17712869]
24. Sinharay S, Randtke EA, Jones KM, Howison CM, Chambers SK, et al. 2017 Noninvasive detection of enzyme activity in tumor models of human ovarian cancer using catalyCEST MRI. Magn. Reson. Med. 77: 2005–14 [PubMed: 27221386]
25. Gu K, Xu Y, Li H, Guo Z, Zhu S, et al. 2016 Real-Time Tracking and In Vivo Visualization of β-Galactosidase Activity in Colorectal Tumor with a Ratiometric Near-Infrared Fluorescent Probe. J. Am. Chem. Soc. 138: 5334–40 [PubMed: 27054782]
26. Wunder A, Tung C-H, Mueller-Ladner U, Weissleder R, Mahmood U. 2004 In vivo imaging of protease activity in arthritis: A novel approach for monitoring treatment response. Arthritis Rheum. 50: 2459–65 [PubMed: 15334458]
27. Rosell A, Ortega-Aznar A, Alvarez-Sabín J, Fernández-Cadenas I, Ribó M, et al. 2006 Increased Brain Expression of Matrix Metalloproteinase-9 After Ischemic and Hemorrhagic Human Stroke. Stroke 37: 1399–406 [PubMed: 16690896]
28. Breckwoldt MO, Chen JW, Stangenberg L, Aikawa E, Rodriguez E, et al. 2008 Tracking the inflammatory response in stroke in vivo by sensing the enzyme myeloperoxidase. Proc. Natl. Acad. Sci. U. S. A. 105: 18584–89, S84/1-S84/3 [PubMed: 19011099]
29. Klohs J, Baeva N, Steinbrink J, Bourayou R, Boettcher C, et al. 2009 In vivo near-infrared fluorescence imaging of matrix metalloproteinase activity after cerebral ischemia. J. Cereb. Blood Flow Metab. 29: 1284–92 [PubMed: 19417756]
30. Rohnert P, Schmidt W, Emmerlich P, Goihl A, Wrenger S, et al. 2012 Dipeptidyl peptidase IV, aminopeptidase N and DPIV/APN-like proteases in cerebral ischemia. J Neuroinflammation 9: 44 [PubMed: 22373413]
31. Asanuma D, Sakabe M, Kamiya M, Yamamoto K, Hiratake J, et al. 2015 Sensitive β-galactosidase-targeting fluorescence probe for visualizing small peritoneal metastatic tumours in vivo. 6: 6463
32. Weissleder R, Tung C-H, Mahmood U, Bogdanov jr A,. 1999 In vivo imaging of tumors with protease-activated near-infrared fluorescent probes. Nat. Biotechnol. 17: 375–78 [PubMed: 10207887]
33. Galis ZS, Sukhova GK, Lark MW, Libby P. 1994 Increased expression of matrix metalloproteinases and matrix degrading activity in vulnerable regions of human atherosclerotic plaques. Journal of Clinical Investigation 94: 2493 [PubMed: 7989608]
34. Galis ZS, Sukhova GK, Libby P. 1995 Microscopic localization of active proteases by in situ zymography: detection of matrix metalloproteinase activity in vascular tissue. The FASEB Journal 9: 974–80 [PubMed: 7615167]
35. Vandooren J, Geurts N, Martens E, Van den Steen PE, Opdenakker G. 2013 Zymography methods for visualizing hydrolytic enzymes. Nature methods 10: 211–20 [PubMed: 23443633]
36. Gawlak M, Górkiewicz T, Gorlewicz A, Konopacki FA, Kaczmarek L, Wilczynski GM. 2009 High resolution in situ zymography reveals matrix metalloproteinase activity at glutamatergic synapses. Neuroscience 158: 167–76 [PubMed: 18588950]
37. Gillespie JW, Best CJM, Bichsel VE, Cole KA, Greenhut SF, et al. 2002 Evaluation of non-formalin tissue fixation for molecular profiling studies. The American journal of pathology 160: 449–57 [PubMed: 11839565]
38. Hadler-Olsen E, Kanapathippillai P, Berg E, Svineng G, Winberg J-O, Uhlin-Hansen L. 2010 Gelatin in situ zymography on fixed, paraffin-embedded tissue: zinc and ethanol fixation preserve enzyme activity. J. Histochem. Cytochem. 58: 29–39 [PubMed: 19755718]
39. Wiera G, Nowak D, Van Hove I, Dziegiel P, Moons L, Mozrzymas JW. 2017 Mechanisms of NMDA receptor-and voltage-gated L-type calcium channel-dependent hippocampal LTP critically rely on proteolysis that is mediated by distinct metalloproteinases. Journal of Neuroscience 37: 1240–56 [PubMed: 28069922]
40. Bremer C, Tung C-H, Weissleder R. 2001 In vivo molecular target assessment of matrix metalloproteinase inhibition. Nature medicine 7: 743

41. Tung C-H, Mahmood U, Bredow S, Weissleder R. 2000 In vivo imaging of proteolytic enzyme activity using a novel molecular reporter. Cancer Res. 60: 4953–58 [PubMed: 10987312]
42. Kircher MF, Weissleder R, Josephson L. 2004 A Dual Fluorochrome Probe for Imaging Proteases. Bioconjugate Chem. 15: 242–48
43. Keow JY, Herrmann KM, Crawford BD. 2011 Differential in vivo zymography: A method for observing matrix metalloproteinase activity in the zebrafish embryo. Matrix Biol. 30: 169–77 [PubMed: 21292002]
44. Jessen JR. 2015 Recent advances in the study of zebrafish extracellular matrix proteins. Developmental Biology 401: 110–21 [PubMed: 25553981]
45. Lee J, Bogyo M. 2010 Development of Near-Infrared Fluorophore (NIRF)-Labeled Activity-Based Probes for in Vivo Imaging of Legumain. ACS Chem. Biol. 5: 233–43 [PubMed: 20017516]
46. Alger JR, Shulman RG. 1984 NMR studies of enzymic rates in vitro and in vivo by magnetization transfer. Q. Rev. Biophys. 17: 83–124 [PubMed: 6091170]
47. Brindle KM. 1988 NMR methods for measuring enzyme kinetics in vivo. Progress in Nuclear Magnetic Resonance Spectroscopy 20: 257–93
48. Rackayova V, Cudalbu C, Pouwels PJW, Braissant O. 2017 Creatine in the central nervous system: From magnetic resonance spectroscopy to creatine deficiencies. Analytical Biochemistry 529: 144–57 [PubMed: 27840053]
49. Campbell-Burk SL, Jones KA, Shulman RG. 1987 Phosphorus-31 NMR saturation-transfer measurements in Saccharomyces cerevisiae: characterization of phosphate exchange reactions by iodoacetate and antimycin A inhibition. Biochemistry 26: 7483–92 [PubMed: 3322400]
50. Kanamori K 2017 In vivo N-15 MRS study of glutamate metabolism in the rat brain. Analytical Biochemistry 529: 179–92 [PubMed: 27580850]
51. Kanamori K, Ross BD. 2005 Suppression of glial glutamine release to the extracellular fluid studied in vivo by NMR and microdialysis in hyperammonemic rat brain. Journal of Neurochemistry 94: 74–85 [PubMed: 15953351]
52. Dona AC, Kyriakides M, Scott F, Shephard EA, Varshavi D, et al. 2016 A guide to the identification of metabolites in NMR-based metabonomics/metabolomics experiments. Computational and Structural Biotechnology Journal 14: 135–53 [PubMed: 27087910]
53. Moats RA, Fraser SE, Meade TJ. 1997 A “smart” magnetic resonance imaging agent that reports on specific enzymic activity. Angew. Chem., Int. Ed. Engl. 36: 726–28
54. Louie AY, Huber MM, Ahrens ET, Rothbacher U, Moats R, et al. 2000 In vivo visualization of gene expression using magnetic resonance imaging. Nat. Biotechnol. 18: 321–25 [PubMed: 10700150]
55. Zhao M, Josephson L, Tang Y, Weissleder R. 2003 Magnetic sensors for protease assays. Angew. Chem., Int. Ed. 42: 1375–78
56. Liu L, Kodibagkar VD, Yu J-X, Mason RP. 2007 19F-NMR detection of lacZ gene expression via the enzymic hydrolysis of 2-fluoro-4-nitrophenyl β-D-galactopyranoside in vivo in PC3 prostate tumor xenografts in the mouse. FASEB J. 21: 2014–19, 10.1096/fj.06-7366lsf [PubMed: 17351127]
57. De Leon-Rodriguez LM, Lubag AJM, Malloy CR, Martinez GV, Gillies RJ, Sherry AD. 2009 Responsive MRI Agents for Sensing Metabolism in Vivo. Acc. Chem. Res. 42: 948–57 [PubMed: 19265438]
58. Terreno E, Delli Castelli D, Viale A, Aime S. 2010 Challenges for Molecular Magnetic Resonance Imaging. Chem. Rev.*(Washington, DC, U. S.)* 110: 3019–42
59. Matsumoto Y, Jasanoff A. 2013 Metalloprotein-based MRI probes. FEBS Lett. 587: 1021–29 [PubMed: 23376346]
60. Vinogradov E, Sherry AD, Lenkinski RE. 2013 CEST: From basic principles to applications, challenges and opportunities. J. Magn. Reson. 229: 155–72 [PubMed: 23273841]
61. Hingorani DV, Yoo B, Bernstein AS, Pagel MD. 2014 Detecting Enzyme Activities with Exogenous MRI Contrast Agents. *Chem.*- Eur. J. 20: 9840–50 [PubMed: 24990812]
62. Karas MB D; Bahr U; Hillenkamp F 1987 Matrix-assisted ultraviolet laser desorption of non-volatile compounds. Int J Mass Spectrom Ion Process 78: 53–68

63. Greis KD. 2007 Mass spectrometry for enzyme assays and inhibitor screening: an emerging application in pharmaceutical research. Mass Spectrom. Rev. 26: 324–39 [PubMed: 17405133]
64. de Rond T, Danielewicz M, Northen T. 2015 High throughput screening of enzyme activity with mass spectrometry imaging. Curr. Opin. Biotechnol. 31: 1–9 [PubMed: 25129648]
65. OuYang C, Chen B, Li L. 2015 High throughput in situ DDA analysis of neuropeptides by coupling novel multiplex mass spectrometric imaging (MSI) with gas-phase fractionation. Journal of The American Society for Mass Spectrometry 26: 1992–2001 [PubMed: 26438126]
66. Grobe N, Elased KM, Cool DR, Morris M. 2012 Mass spectrometry for the molecular imaging of angiotensin metabolism in kidney. Am. J. Physiol. 302: E1016–E24
67. Javelot HM M; Garnier S; Rougeot C 2010 Human Opiorphin is a Nautrally Occurring Antidepressant Acting Selectively on Enkephalin-Dependent δ-Opioid Pathways. Journal of Physiology and Pharmacology 61: 355–62 [PubMed: 20610867]
68. Yang J, Chaurand P, Norris JL, Porter NA, Caprioli RM. 2012 Activity-Based Probes Linked with Laser-Cleavable Mass Tags for Signal Amplification in Imaging Mass Spectrometry: Analysis of Serine Hydrolase Enzymes in Mammalian Tissue. Anal. Chem. *(Washington, DC, U. S.)* 84: 3689–95
69. Koehbach J, Gruber CW, Becker C, Kreil DP, Jilek A. 2016 MALDI TOF/TOF-Based Approach for the Identification of d- Amino Acids in Biologically Active Peptides and Proteins. J Proteome Res 15: 1487–96 [PubMed: 26985971]
70. Livnat I, Tai HC, Jansson ET, Bai L, Romanova EV, et al. 2016 A d-Amino Acid-Containing Neuropeptide Discovery Funnel. Anal Chem 88: 11868–76 [PubMed: 27788334]
71. Marfey P 1984 Determination of D-amino Acids. II. Use of a Bifunctional Reagent, 1,5-difluoro-2,4-dinitrobenzene. Carlsberg Res. Commun. 49: 591–96
72. Bhushan R, Bruckner H. 2004 Marfey's reagent for chiral amino acid analysis: a review. Amino Acids 27: 231–47 [PubMed: 15503232]
73. Ungerstedt U 1984 Measurement of neurotransmitter release by intercranial dialysis In Measurement of neurotransmitter release in vivo, ed. Marsden CA, pp. 81–105. New York: Wiley
74. Lee WH, Ngernsutivorakul T, Mabrouk OS, Wong J-MT, Dugan CE, et al. 2016 Microfabrication and in Vivo Performance of a Microdialysis Probe with Embedded Membrane. Analytical Chemistry 88: 1230–37 [PubMed: 26727611]
75. Newcomb R, Pierce AR, Kano T, Meng W, Bosque-Hamilton P, et al. 1998 Characterization of mitochondrial glutaminase and amino acids at prolonged times after experimental focal cerebral ischemia. Brain Res. 813: 103–11 [PubMed: 9824679]
76. Sato T, Obata T, Yamanaka Y, Arita M. 1998 Effects of lysophosphatidylcholine on the production of interstitial adenosine via protein kinase C-mediated activation of ecto-5'-nucleotidase. Br. J. Pharmacol. 125: 493–98 [PubMed: 9806332]
77. Obata T 2002 Adenosine production and its interaction with protection of ischemic and reperfusion injury of the myocardium. Life Sci. 71: 2083–103 [PubMed: 12204768]
78. Wang Y, Zagorevski DV, Lennartz MR, Loegering DJ, Stenken JA. 2009 Detection of in vivo matrix metalloproteinase activity using microdialysis sampling and liquid chromatography/mass spectrometry. Anal Chem 81: 9961–71 [PubMed: 19904964]
79. Kozai TDY, Jaquins-Gerstl AS, Vazquez AL, Michael AC, Cui XT. 2015 Brain Tissue Responses to Neural Implants Impact Signal Sensitivity and Intervention Strategies. ACS Chemical Neuroscience 6: 48–67 [PubMed: 25546652]
80. Jaquins-Gerstl A, Shu Z, Zhang J, Liu Y, Weber SG, Michael AC. 2011 Effect of dexamethasone on gliosis, ischemia, and dopamine extraction during microdialysis sampling in brain tissue. Analytical chemistry 83: 7662–67 [PubMed: 21859125]
81. Nesbitt KM, Jaquins-Gerstl A, Skoda EM, Wipf P, Michael AC. 2013 Pharmacological mitigation of tissue damage during brain microdialysis. Analytical chemistry 85: 8173–79 [PubMed: 23927692]
82. Nesbitt KM, Varner EL, Jaquins-Gerstl A, Michael AC. 2014 Microdialysis in the Rat Striatum: Effects of 24 h Dexamethasone Retrodialysis on Evoked Dopamine Release and Penetration Injury. ACS chemical neuroscience 6: 163–73 [PubMed: 25491242]

83. Kozai TDY, Jaquins-Gerstl AS, Vazquez AL, Michael AC, Cui XT. 2016 Dexamethasone retrodialysis attenuates microglial response to implanted probes in vivo. Biomaterials 87: 157–69 [PubMed: 26923363]
84. Varner EL, Leong CL, Jaquins-Gerstl A, Nesbitt KM, Boutelle MG, Michael AC. 2017 Enhancing Continuous Online Microdialysis using Dexamethasone: Measurement of Dynamic Neurometabolic Changes during Spreading Depolarization. ACS Chemical Neuroscience
85. Albiston AL, Mustafa T.; McDowall.; Mendelsohn FAO.; Lee J.; Chai SY. 2003 AT4 receptor is insulin-regulated membrane aminopeptidase: potential mechanisms of memory enhancement. TRENDS in Endocrinology and Metabolism 14: 72–77 [PubMed: 12591177]
86. Fernando RN, Albiston AL, Chai SY. 2008 The insulin-regulated aminopeptidase IRAP is colocalised with GLUT4 in the mouse hippocampus--potential role in modulation of glucose uptake in neurones? Eur J Neurosci 28: 588–98 [PubMed: 18702730]
87. De Bundel D, Smolders I, Yang R, Albiston AL, Michotte Y, Chai SY. 2009 Angiotensin IV and LVV-haemorphin 7 enhance spatial working memory in rats: effects on hippocampal glucose levels and blood flow. Neurobiol Learn Mem 92: 19–26 [PubMed: 19233301]
88. De Bundel D, Demaegdt H, Lahoutte T, Caveliers V, Kersemans K, et al. 2010 Involvement of the AT1 receptor subtype in the effects of angiotensin IV and LVV-haemorphin 7 on hippocampal neurotransmitter levels and spatial working memory. J Neurochem 112: 1223–34 [PubMed: 20028450]
89. Fletcher HJ, Stenken JA. 2008 An in vitro comparison of microdialysis relative recovery of Met- and Leu-enkephalin using cyclodextrins and antibodies as affinity agents. Anal Chim Acta 620: 170–5 [PubMed: 18558138]
90. Duo J, Stenken JA. 2011 In vitro and in vivo affinity microdialysis sampling of cytokines using heparin-immobilized microspheres. Anal. Bioanal. Chem. 399: 783–93 [PubMed: 21052646]
91. Schmerberg CM, Li L. 2013 Mass Spectrometric Detection of Neuropeptides Using Affinity-Enhanced Microdialysis with Antibody-Coated Magnetic Nanoparticles. Anal. Chem. *(Washington, DC, U. S.)* 85: 915–22 [PubMed: 23249250]
92. Freed AL, Cooper JD, Davies MI, Lunte SM. 2001 Investigation of the metabolism of substance P in rat striatum by microdialysis sampling and capillary electrophoresis with laser-induced fluorescence detection. J. Neurosci. Methods 109: 23–29 [PubMed: 11489296]
93. Reed B, Bidlack JM, Chait BT, Kreek MJ. 2008 Extracellular biotransformation of β-endorphin in rat striatum and cerebrospinal fluid. J. Neuroendocrinol. 20: 606–16 [PubMed: 18363801]
94. Reed B, Zhang Y, Chait BT, Kreek MJ. 2003 Dynorphin A(1–17) biotransformation in striatum of freely moving rats using microdialysis and matrix-assisted laser desorption/ionization mass spectrometry. J. Neurochem. 86: 815–23 [PubMed: 12887680]
95. Klintenberg R, Andren PE. 2005 Altered extracellular striatal in vivo biotransformation of the opioid neuropeptide dynorphin A(1–17) in the unilateral 6-OHDA rat model of Parkinson's disease. J. Mass Spectrom. 40: 261–70 [PubMed: 15706626]
96. Stragier B, Sarre S, Vanderheyden P, Vauquelin G, Fournie-Zaluski MC, et al. 2004 Metabolism of angiotensin II is required for its in vivo effect on dopamine release in the striatum of the rat. J Neurochem 90: 1251–7 [PubMed: 15312180]
97. Zhang H, Stoeckli M, Andren PE, Caprioli RM. 1999 Combining solid-phase preconcentration, capillary electrophoresis and off-line matrix-assisted laser desorption/ionization mass spectrometry: intracerebral metabolic processing of peptide Ein vivo. Journal of Mass Spectrometry 34: 377–83 [PubMed: 10226364]
98. Ou Y, Wu J, Sandberg M, Weber SG. 2014 Electroosmotic perfusion of tissue: sampling the extracellular space and quantitative assessment of membrane-bound enzyme activity in organotypic hippocampal slice cultures. Analytical and bioanalytical chemistry 406: 6455–68 [PubMed: 25168111]
99. Hamsher AE, Xu H, Guy Y, Sandberg M, Weber SG. 2010 Minimizing tissue damage in electroosmotic sampling. Analytical chemistry 82: 6370–76 [PubMed: 20698578]
100. Gogolla N, Galimberti I, DePaola V, Caroni P. 2006 Preparation of organotypic hippocampal slice cultures for long-term live imaging. Nature protocols 1: 1165–71 [PubMed: 17406399]

101. Mentlein RG B; Schmidt WE 1993 Dipeptidyl-peptidase IV hydrolyses gastric inhibitory polypeptide, glucagon-likepeptide-l(7–36)amide, peptidehistidinemethionine and is responsible for their degradation in human serum. Eur. J. Biochem. 214: 829–35 [PubMed: 8100523]
102. Roques BPN F; Dauge V; Fournie-Zaluski MC.; Beaumont A. 1993 Neutral Endopeptidase 24.11: Structure, Inhibition, and Experimental and Clinical Pharmacology. Pharmacological Reviews 45: 87–146 [PubMed: 8475170]
103. Thielitz A, Ansorge S, Bank U, Tager M, Wrenger S, et al. 2008 The ectopeptidases dipeptidyl peptidase IV (DP IV) and aminopeptidase N (APN) and their related enzymes as possible targets in the treatment of skin diseases. Front. Biosci. 13: 2364–75 [PubMed: 17981718]
104. Wu J, Sandberg M, Weber SG. 2013 Integrated electroosmotic perfusion of tissue with online microfluidic analysis to track the metabolism of cystamine, pantethine, and coenzyme A. *Analytical chemistry* 85: 12020–27 [PubMed: 24215585]
105. Wu J, Xu K, Landers JP, Weber SG. 2013 An in situ measurement of extracellular cysteamine, homocysteine, and cysteine concentrations in organotypic hippocampal slice cultures by integration of electroosmotic sampling and microfluidic analysis. Analytical chemistry 85: 3095–103 [PubMed: 23330713]
106. Wu J, Ferrance JP, Landers JP, Weber SG. 2010 Integration of a precolumn fluorogenic reaction, separation, and detection of reduced glutathione. Analytical chemistry 82: 7267–73 [PubMed: 20698502]
107. Xu H, Guy Y, Hamsher A, Shi G, Sandberg M, Weber SG. 2010 Electroosmotic sampling. Application to determination of ectopeptidase activity in organotypic hippocampal slice cultures. Analytical chemistry 82: 6377–83 [PubMed: 20669992]
108. Rupert AE, Ou Y, Sandberg M, Weber SG. 2013 Electroosmotic Push–Pull Perfusion: Description and Application to Qualitative Analysis of the Hydrolysis of Exogenous Galanin in Organotypic Hippocampal Slice Cultures. ACS chemical neuroscience 4: 838–48 [PubMed: 23614879]
109. Ou Y, Weber SG. 2017 Numerical Modeling of Electroosmotic Push–Pull Perfusion and Assessment of Its Application to Quantitative Determination of Enzymatic Activity in the Extracellular Space of Mammalian Tissue. Analytical Chemistry
110. Zini S, Roisin M-P, Armengaud C, Ben-Ari Y. 1993 Effect of potassium channel modulators on the release of glutamate induced by ischaemic-like conditions in rat hippocampal slices. Neuroscience letters 153: 202–05 [PubMed: 8100991]
111. Elliott-Hunt CR, Marsh B, Bacon A, Pope R, Vanderplank P, Wynick D. 2004 Galanin acts as a neuroprotective factor to the hippocampus. Proceedings of the National Academy of Sciences of the United States of America 101: 5105–10 [PubMed: 15041741]
112. Beal SL. 1982 On the solution to the Michaelis-Menten equation. Journal of pharmacokinetics and biopharmaceutics 10: 109–19 [PubMed: 7069576]
113. Golicnik M 2011 Explicit analytic approximations for time-dependent solutions of the generalized integrated Michaelis-Menten equation. Anal. Biochem. 411: 303–05 [PubMed: 21241654]
114. Ou Y, Weber SG. 2017 Higher aminopeptidase activity determined by electroosmotic push-pull perfusion contributes to selective vulnerability of the hippocampal CA1 region to oxygen glucose deprivation. *ACS Chemical Neuroscience*: Submitted.
115. Rupert AE, Ou Y, Sandberg M, Weber SG. 2013 Assessment of Tissue Viability Following Electroosmotic Push–Pull Perfusion from Organotypic Hippocampal Slice Cultures. ACS chemical neuroscience 4: 849–57 [PubMed: 23639590]
116. Jaquins-Gerstl A, Michael AC. 2015 A review of the effects of FSCV and microdialysis measurements on dopamine release in the surrounding tissue. Analyst 140: 3696–708 [PubMed: 25876757]

Summary Points

1. Broadly speaking, there are two goals justifying the measurement of enzyme activity in/ex vivo, namely discovery or characterization of damaged or diseased tissue, for example in arthritis or cancer, and biology, biochemistry, or neurochemistry.
2. Fluorescence techniques applied to appropriately prepared tissue slices can provide a quantitative histological picture of enzyme activity at diffraction limited spatial resolution. Near IR fluorophores have been adapted for in vivo work.
3. Activity-based probes specifically target active enzymes for in vivo imaging.
4. Magnetic-resonance based methods have been applied successfully to both biochemical investigations and imaging.
5. MALDI mass spectrometry has high spatial resolution, can identify novel natural substrates and products, and provide images.
6. Microdialysis is a sampling technique that provides quantitative information for a variety enzymes in vivo by monitoring the increase and decrease of substrate and product concentrations in the microdialsysate.
7. Electroosmotic sampling ex vivo coupled to microfluidic fluorogenic reaction/capillary electrophoresis separation/laser-induced fluorescence to elucidate details CoA catabolism, providing V_{max} and K_m for membrane-bound enzyme activity.
8. Electroosmotic push-pull perfusion perfuses tissue extracellular space with natural substrates and provides V_{max} and K_m of membrane-bound enzyme activity with good (100–300 μm) spatial resolution. The integrated Michaelis Menten equation must be used.

Future Issues

Those who seek to determine the presence and extent of tissue in a pathological state have made significant progress. Progress is expected in improving the sensitivity of the method – the ability to detect smaller abnormalities sooner - and should decrease the time required for imaging. The creativity in the design and synthesis of synthetic, signal-producing substrates has been remarkable, so the outlook for improvements is bright.

Several techniques described here have been applied to biochemical, developmental, and neurological questions. Magnetic resonance approaches are the most mature due to their clinical applications while the application of physical probes to the problems of determining enzyme activity in/ex vivo is still in early stages. Some things to look for in this arena are:

- How well do samples collected with physical probes represent the unperturbed, in vivo environment? How can this alteration and damage be eliminated? There is progress being made in microdialysis by the Michael and Cui groups (79, 83, 116). Nonetheless, this is, and will always be, an important direction for research.
- A related direction is to know how ex vivo measurements relate to in vivo measurements. When using chemical probes with the right properties, e.g. with activity-based fluorogenic probes, this can be done straightforwardly. But with physical probes and techniques like MALDI-mass spectrometry, more proof of concept experiments are required.
- The field will develop measurements that explore multiple steps in an enzyme-catalyzed reaction pathway, garnering information about the enzymatic rates. The field of magnetic resonance has profitably employed a pulse-chase type experiment to infer rates from steady-state systems.
- The electroosmotic perfusion techniques have demonstrated the ability to obtain quite good quantitative characterization of ectoenzyme activity with 100 – 200 μm resolution. As the analytical assessment of the activity of enzymes comes from chromatography and microfluidic capillary electrophoresis, it is conceivable to measure multiple products that arise from a substrate and thus characterize more than one enzyme rate.

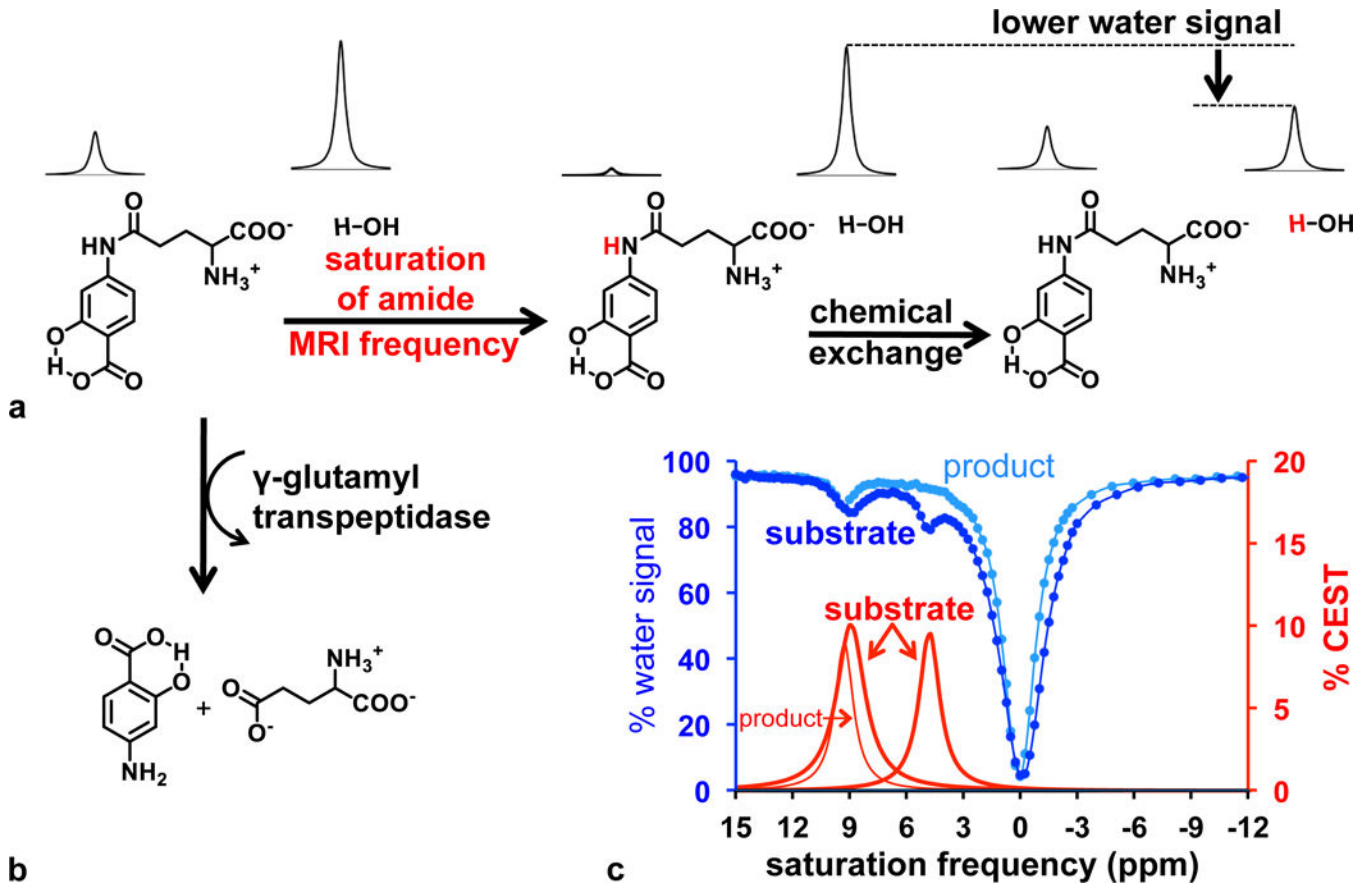

Figure 1.

Protons differ in their ability to exchange excited protons with water, their relaxivity (20). Exciting high relaxivity protons on a compound (panel a) has the effect of indirectly exciting water protons because of proton exchange. The signal from water thus appears more saturated when the said compound is present and being excited in comparison to the absence of the compound. A negative peak in the “%water signal” appears at the chemical shift (with respect to water) of the high relaxivity proton (panel c). When the high-relaxivity amide is converted to the lower relaxivity amine, the effect decreases (panel b). The phenolic proton has high relaxivity but at a different chemical shift and its relaxivity is relatively unaffected by hydrolysis of the amide (panel b). This proton acts as an internal standard or control against which the amide proton signal can be compared. Adapted from Sinharay et al. 2017 Magnetic Resonance in Medicine 77: 2005–2014. Copyright 2016 International Society for Magnetic Resonance in Medicine.

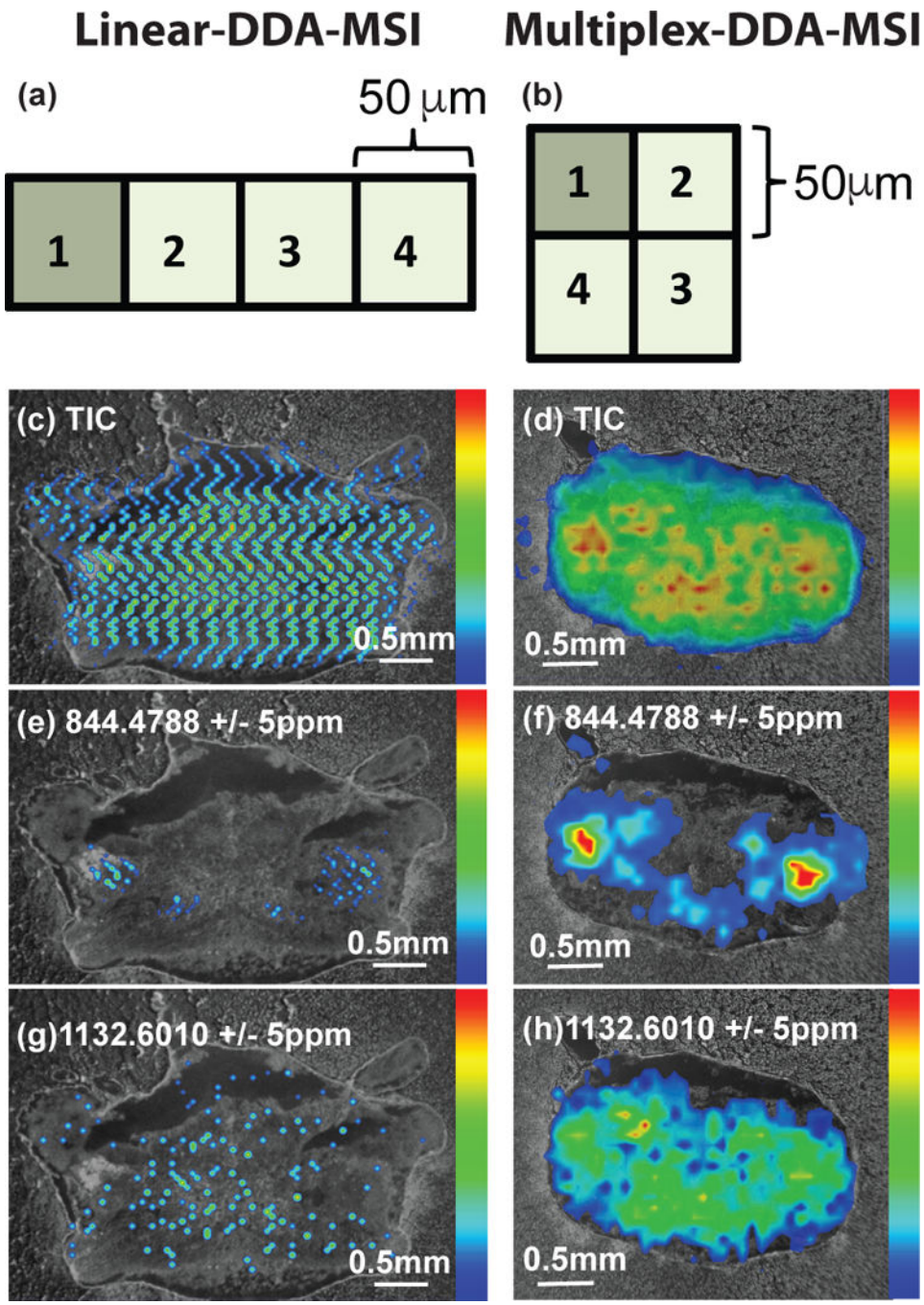

Figure 2.

Comparison of DDA steps in linear (a) versus spiral (b) MSI. In both cases, Step 1 is a full scan MS for the desired mass range and Steps 2–4 are sequential fragmentations of the 3 most intense ions in Step 1. The total ion chromatograms (TIC) of blue crab commissural ganglion tissue slices illustrate how spatial resolution is maintained with the spiral (d) method compared to the linear (c). Using the spiral method (f & h), the authors were able to map the distribution of the peptides HL/IGSL/IYRamide (m/z 844.4788) (e & f) and VSHNNFLRFamide (m/z 1132.6010) (g &h) whereas the linear method (e & g) revealed

only a fraction of areas where the peptides were located. Reprinted with permission from OuYang, et al. 2015 Journal of the American Society for Mass Spectrometry 26: 1992–2001. Copyright 2015 American Society for Mass Spectrometry.

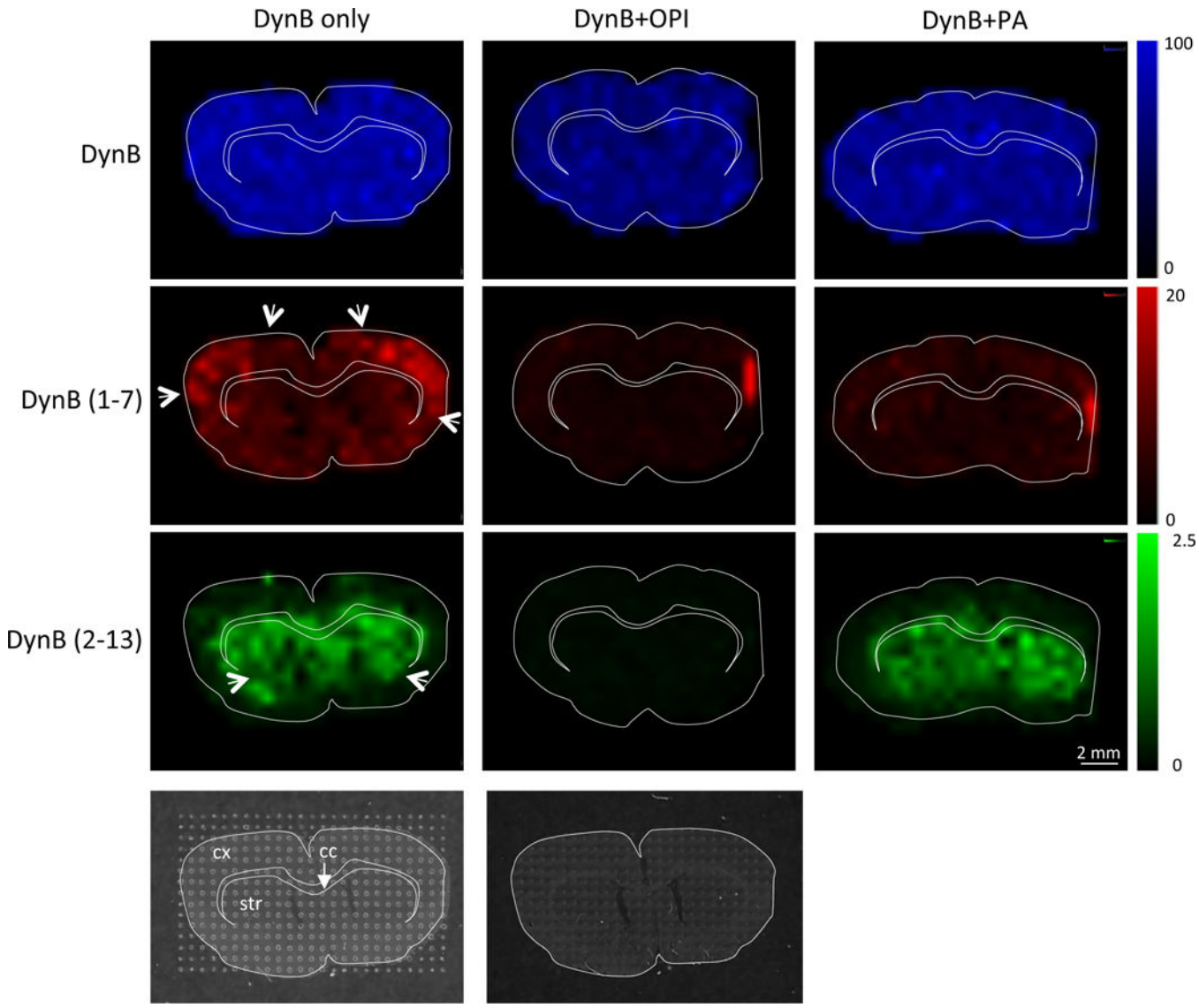

Figure 3.

Mass spectroscopic images of rat brain slices containing exogenously applied dynorphin B (DynB) in the absence (left) and presence (middle, right) of inhibitors. While Dyn B was hydrolyzed throughout the regions sampled, the fragments DynB (1-7) were more prevalent in the cortex (cx, indicated by arrows) whereas Dyn B (2-13) showed the highest intensities in the striatum (str). The inhibitor opiorphin (OPI) blocked nearly all formation of DynB (1-7) and DynB (2-13) whereas phosphoramidon (PA) prevented the formation of DynB (1-7) but did not appear to affect DynB (2-13) formation. The area of relatively higher intensity in the top, right corner of the DynB (1-7) images is due to a fold in the tissue. The bottom panel illustrates the tissue structures, including the corpus callosum (cc) used for region identification before (left) and after (right) matrix application. Reprinted with permission from Bivehed, E., et al. 2017. Peptides 87: 20–27. Copyright 2016 Bivehed, E. et al under Creative Commons license https://creativecommons.org/licenses/by-nc-nd/4.0/.

Published by Elsevier Inc. DOI 10.1016/j.peptides.2016.11.006. Cannot be modified without permission from journal.

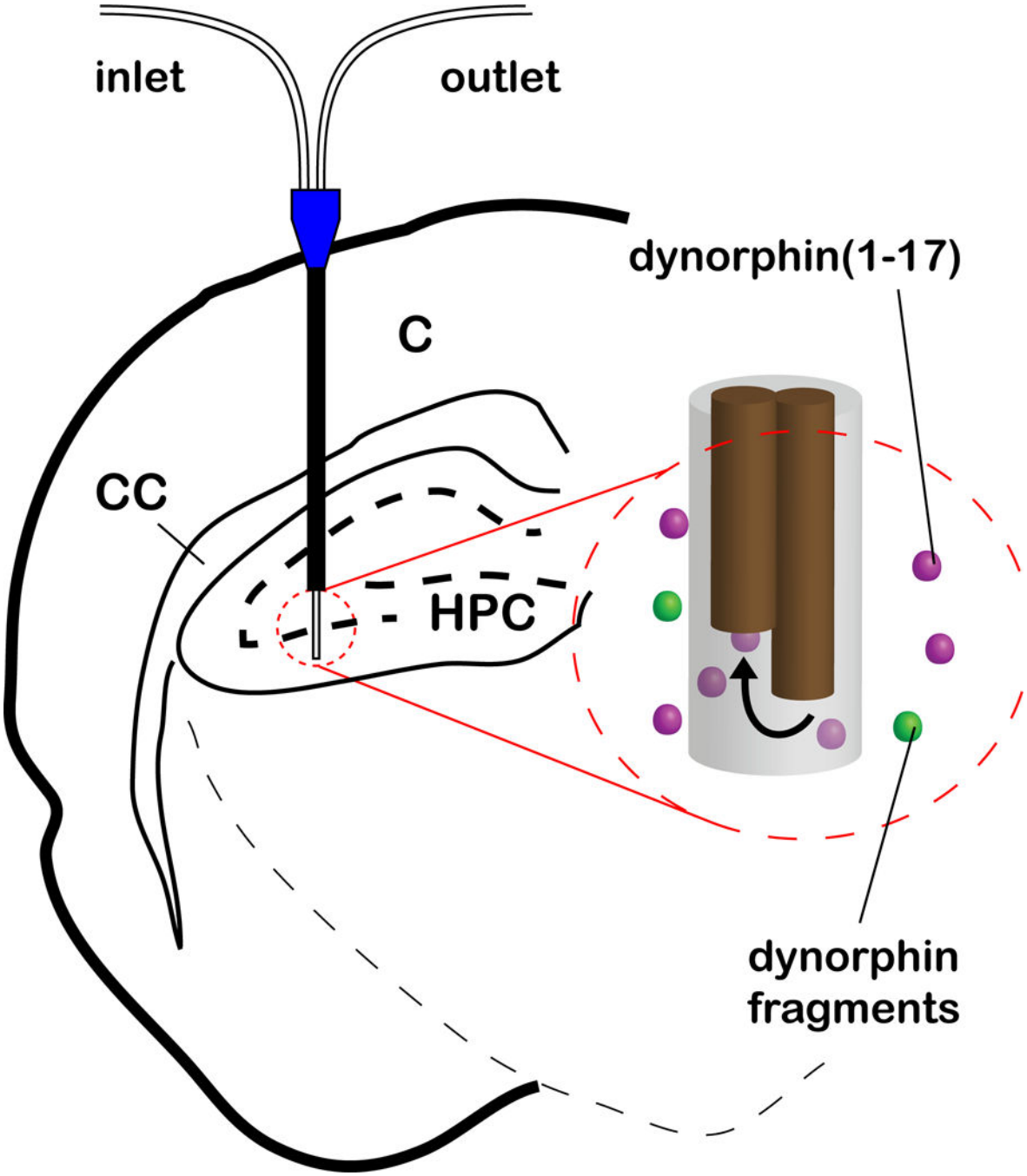

Figure 4.

Schematic showing a typical microdialysis experiment, in which the probe is implanted into the rat hippocampus. Inside the membrane, there is usually a concentric or side-by-side (shown) design of the inlet and outlet capillaries. Arrow indicates flow of perfusion fluid inside the membrane. Any species in the surrounding ECS, such as dynorphins and dynorphin fragments can diffuse through the membrane, be collected and quantified. C – cortex; CC – corpus callosum; HPC – hippocampus. Figure not drawn to scale.

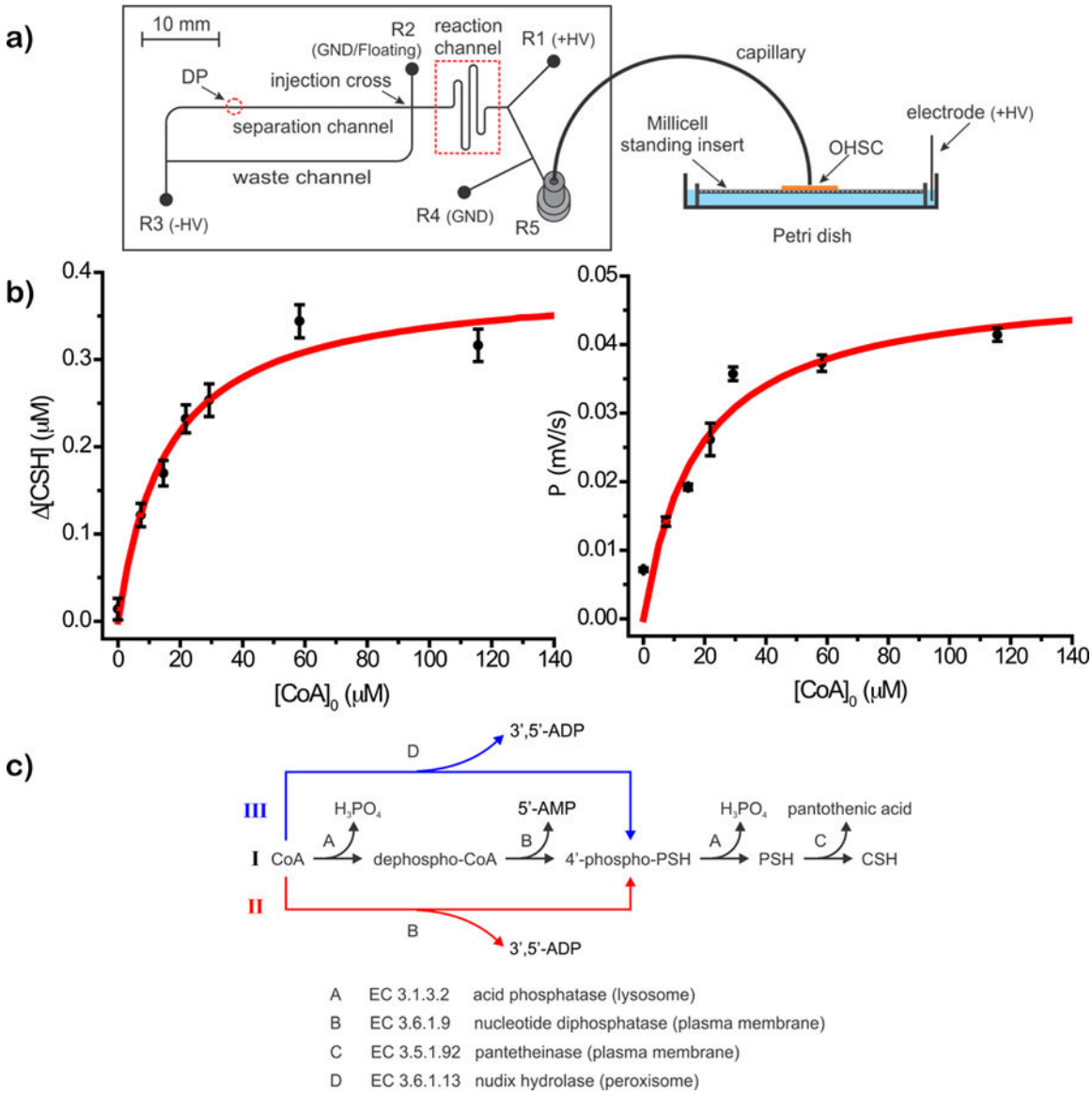

Figure 5.

(a) Schematic of the online electroosmotic sampling experiment with microfluidic chip. The organotypic hippocampal slice culture (OHSC) sits upon a membrane insert on which it is grown. A sampling capillary is placed above the tissue while the other (distal) end is inserted into R5 reservoir of the microfluidic device. R1 contains ThoGlo-1, a thiol-specific reagent, R2 and R3 contains running buffer, and R4 contains Tris-HCl buffer. The thiol compounds collected from OHSC is allowed to react with ThioGlo-1 in the reaction channel, followed by separation via capillary electrophoresis. DP = detection point by laser-induced fluorescence. (b) Nonlinear fits of cysteamine (CSH) and pantetheine (P) generated from CoA hydrolysis. (c) Three proposed (I, II, III) degradation pathways of CoA. PSH = pantetheine. Adapted with permission from Wu et al. 2013. Analytical Chemistry 85: 3095–103 and Wu et al. 2013 Analytical Chemistry 85: 12020–27. Copyright 2013 American Chemical Society.

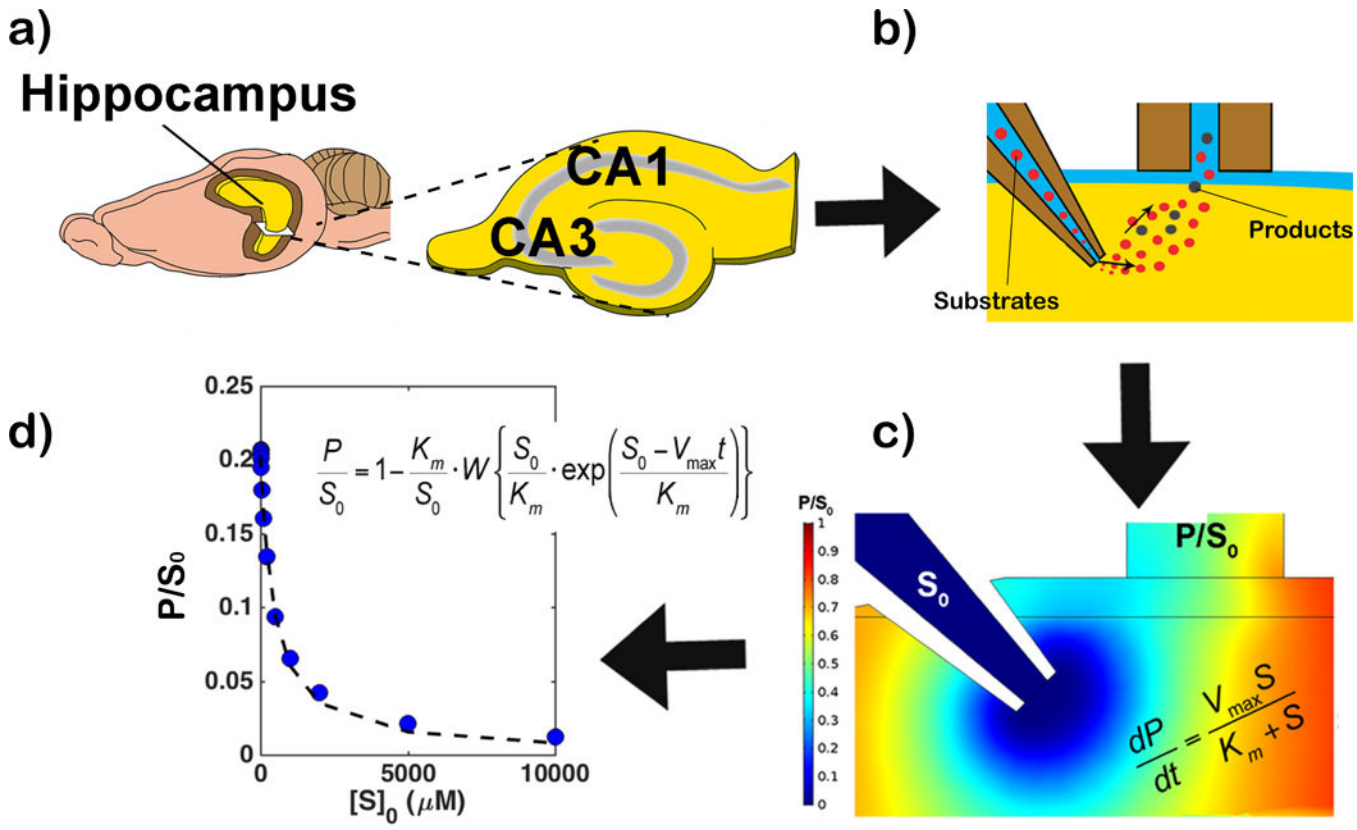

Figure 6.

Schematic illustrating a typical EOPPP experiment. (a) The CA1 and CA3 regions of the rat OHSCs are perfused with exogenous (b) Leu-enkephalin (YGGFL) and internal standard ($^{D}Y^{D}AG^{D}F^{D}L$) at the same concentration, S_0, through a pulled fused silica capillary. YGGFL is hydrolyzed in the ECS by membrane-bound aminopeptidases with the major product being GGFL. YGGFL, $^{D}Y^{D}AG^{D}F^{D}L$ and GGFL are collected in the sampling capillary and quantified offline using capillary liquid chromatography. (c) Numerical modeling gives estimates of the distribution of product concentration as a ratio to internal standard concentration which is equal to the initial substrate concentration, P/S_0. P/S_0 ratios under quasi-steady-state conditions are seen to vary considerably, making the assumption that the initial substrate concentration is constant untenable. (d) The integrated Michaelis Menten equation is fitted to P/S_0 produced at different S_0 to give estimates of V_{max} and K_m of aminopeptidase activity in the tissue. Adapted from Ou and Weber 2017. Analytical Chemistry 89: 5864–5873. Copyright 2017 American Chemical Society.